This is a post-peer-review, pre-copyedit version of an article published in **2017 19th European Conference on Power Electronics and Applications (EPE'17 ECCE Europe)**. The final authenticated version is available online at: DOI: 10.23919/EPE17ECCEEurope.2017.8098958

Hysteresis modelling of a medium frequency single-phase transformer

Piotr Dworakowski [1,2], Andrzej Wilk [1], Bruno Lefebvre [2]

[1] Faculty of Electrical and Control Engineering, Gdansk University of Technology
ul. Gabriela Narutowicza 11/12
80-233 Gdansk, Poland

[2] SuperGrid Institute
130 rue Leon Blum
69100 Villeurbanne, France
piotr.dworakowski@supergrid-institute.com

Acknowledgements

This work was supported by a grant overseen by the French National Research Agency (ANR) as part of the “Investissements d’Avenir” Program (ANE-ITE-002-01).

Keywords

«Transformer», «Modelling», «High frequency power converter», «High voltage power converters», «DC collector network».

Abstract

The article describes a feedback Preisach hysteresis model equivalent circuit implementation of a medium frequency single-phase transformer being a part of a high power and high efficiency DC-DC converter. The macroscopic models of magnetic hysteresis are introduced and the feedback Preisach model is selected for further analysis. The hysteresis model is developed for a prototype transformer and the hysteresis loops are compared against a measurement. The equivalent circuit implementation of the hysteresis model is proposed and analysed. The equivalent circuit model is validated in no load operation and compared with a measurement.

Introduction

The transmission of electric energy over the long distances is now reserved to High Voltage Direct Current HVDC [1]. Thanks to the technological improvements in the wide bandgap semiconductors as the Silicon Carbide SiC [2] a large number of power applications may move to DC soon. Numerous research projects and some industrial projects target DC-DC power converters as a key component. The DC-DC converters are often proposed for environment friendly applications like: photovoltaic [3], electric vehicles [4], wind power [5], railway traction [6], etc. Together with the power semiconductor development, there has been a significant evolution in passive components like capacitors, inductors and transformers enabling the operation at higher voltage and higher frequency. Since the power converters are used in more and more critical applications involving new technologies, it has revealed a need of precise modelling tool for design and health monitoring.

In this article a medium frequency single-phase transformer is studied taking into account the hysteresis phenomenon of the magnetic material. The transformer is a part of a high efficiency and compact isolated DC-DC converter with nominal power 100 kW, input voltage 1200 Vdc and output voltage 600 Vdc. The converter topology is a Dual Active Bridge [7] with the AC link operating at 20 kHz (Fig. 1). The transformer model is essential when analysing the operation of converters and when optimising the design for high efficiency applications thanks to the robust core loss calculation in different operating conditions.

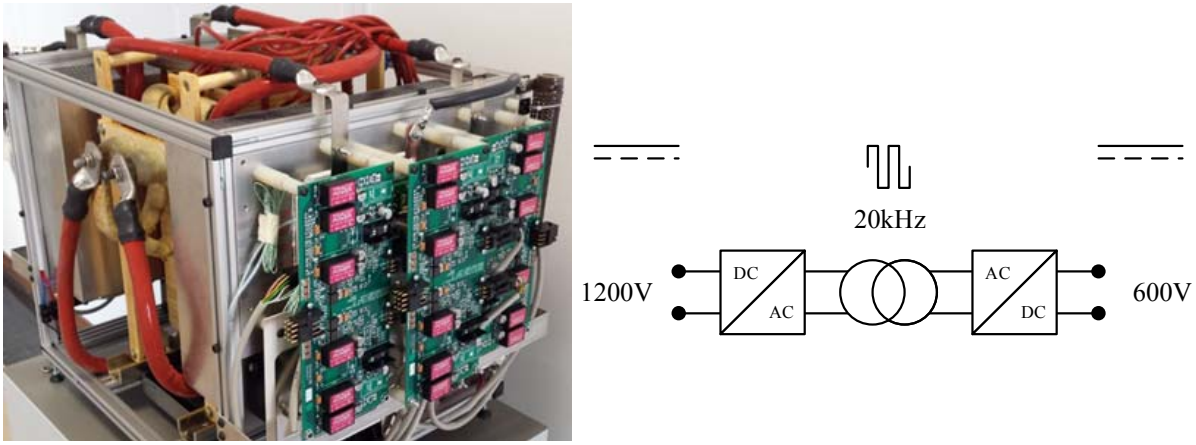

Fig. 1: High efficiency and compact isolated DC-DC 100 kW converter including the medium frequency single-phase transformer: photo (left) and schematics (right)

Medium frequency transformer modelling has to take into account the numerous physical phenomena like skin and proximity effects [8] and capacitive couplings of the windings, and eddy effects and magnetic hysteresis [9] of the core. This article gives the state of the art on the macroscopic models of magnetic hysteresis and proposes the implementation of a feedback Preisach model. The parameters of the model are identified thanks to a measurement on a prototype transformer. The model is validated in a circuit simulation compared against a measurement.

Macroscopic models of magnetic hysteresis

In converter system level analysis the most suitable models of hysteresis are the macroscopic models [10]. So far the most accurate models of hysteresis are the Preisach model (PM) [11] and the Jiles-Atherton model (J-A) [12].
The J-A model can be used in the analysis of coupled electromagnetic, thermal and motion phenomena [13], [14], including the FEM calculations [15]. An algorithm and its implementation was presented in [16] allowing to determine the J-A model parameters. The J-A model is based on reversible and irreversible components of the total magnetization in the magnetic material.
The PM was initially used in the field of magnetism but thanks to its mathematical representation it has been extended to other domains. A mathematical form of the PM was proposed in [17] and further developed in [18]. The PM involves a double integral of Preisach distribution function $\mu(\alpha,\beta)$ allowing to calculate the magnetic flux density B as a function of the magnetic field intensity H. In the PM the magnetic flux density depends on the magnetic field intensity and on the material magnetization history. There have been many modifications of the original PM: generalized PM, moving PM, dynamic PM, vector PM which are presented in [19]. In this article the feedback Preisach model [20], [21] has been used allowing to gain the accuracy in the hysteresis nonlinearity modelling.
This article proposes the development of the medium frequency single-phase transformer circuit model coupled with the generalized scalar Preisach model of hysteresis. The equivalent circuit model uses the common magnetic flux Φ_c as a function of ampere-turns Θ of all coils involving the hysteresis nonlinearity. The Preisach distribution function $\mu(\alpha,\beta)$ is approximated by an analytical formula and the feedback function uses a third order polynomial. The model also includes an equivalent circuit for eddy currents.

The feedback Preisach model of hysteresis

In the classical Preisach model, a ferromagnetic material is made up of an infinite set of magnetic dipoles (hysteresis operators), each having the magnetic characteristics with two separate and randomly distributed properties α and β. Each operator has a rectangular hysteresis loop and it is defined by a mathematical operator $\gamma_{\alpha,\beta}(H)$, as presented in Fig. 2 (left). In the classical Preisach model the relationship between the magnetic field intensity H and the magnetic flux density B is expressed by the integral (1)

$$B = \iint_{\alpha \geq \beta} \mu(\alpha,\beta)\gamma_{\alpha,\beta}(H)\,\mathrm{d}\alpha\mathrm{d}\beta \tag{1}$$

where $\mu(\alpha,\beta)$ is the Preisach distribution function (PDF), being a kind of a material constant defined as a finite weight function having nonzero values within the limits of major hysteresis loop. The PDF $\mu(\alpha,\beta)$ can be also considered as a probability density function where $\mu(\alpha,\beta)\mathrm{d}\alpha\mathrm{d}\beta$ equals the probability that a randomly selected operator has a rectangular loop (α,β). In the feedback Preisach model (FPM) the positive switching field α is replaced by $\alpha+H_f(B)$ and the negative switching field β is replaced by $\beta+H_f(B)$. In this article the hysteresis nonlinearity is proposed to be involved in $\Phi_c(\Theta)$ expression.

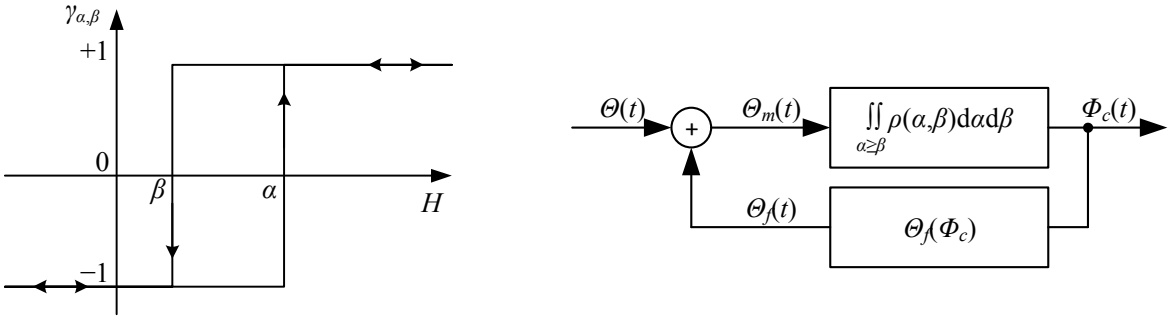

Fig. 2: Rectangular loop of an elementary hysteresis operator (left) and a block diagram of the feedback Preisach model of hysteresis (right)

The FPM can be represented in a block diagram Fig. 2 (right). The upper box represents the classical Preisach transducer [18]. The lower box represents the feedback term $\Theta_f(\Phi_c)$ that adds to the effective magnetomotive force acting on the elementary hysteresis operator. Finally, the FPM can be defined by the equation (2)

$$\begin{aligned} \Phi_c(t) &= \iint_{\alpha \geq \beta} \rho\left[\alpha + \Theta_f(\Phi_c), \beta + \Theta_f(\Phi_c)\right]\gamma_{\alpha,\beta}[\Theta_m(t)]\,\mathrm{d}\alpha\mathrm{d}\beta \\ \Theta_m &= \Theta + \Theta_f(\Phi_c) \end{aligned} \tag{2}$$

where the $\rho(\alpha,\beta,\Theta(\Phi_c))$ is the PDF depending on the common flux Φ_c, the $\gamma_{\alpha,\beta}(\Theta_m)$ describes the rectangular loop of an elementary hysteresis operator.

A circuit simulation of the FPM requires the calculation of $\rho(\alpha,\beta,\Theta(\Phi_c))$ and $\Theta_f(\Phi_c)$. An analytical approach for the calculation of feedback field $H_f(B)$ was proposed in [24] but it is only applicable for relatively small feedback factors. A complete FPM parameter identification procedure was proposed in [25] but a linear feedback function was assumed which limits the use to some materials only. In [26] an nonlinear feedback function $H_f(B)$ was used and the factorisation property of the function $\mu(\alpha,\beta)$ was assumed, again limiting the use to some materials only.

In this article, to approximate the PDF it is proposed a two-dimensional Gauss functional series (3)

$$\rho(\alpha,\beta) = \frac{1}{2\pi}\sum_{n=1}^{N}\frac{A_n}{S_{x,n}S_{y,n}}\exp\left(\frac{-(\alpha+\beta)^2}{2{S_{x,n}}^2}\right)\exp\left(\frac{-(\alpha-\beta)^2}{2{S_{y,n}}^2}\right) \tag{3}$$

where A_n, $S_{x,n}$, and $S_{y,n}$ are constant parameters.

The feedback function is proposed to be a third order polynomial (4)

$$\Theta_f(\Phi_c) = K_1\Phi_c + K_3{\Phi_c}^3 \tag{4}$$

where K_1 and K_3 are constant parameters.

Parameters identification of the feedback Preisach model

The identification of the FPM requires the calculation of A_n, $S_{x,n}$, $S_{y,n}$, K_1 and K_3 parameters. The measurements were carried out on the medium frequency single-phase transformer (Fig. 3). The apparent power of the transformer is 180 kVA, the primary rated voltage is 1200 V and the secondary rated voltage is 600 V. The transformer was designed to operate at the frequency between 17 and 23 kHz with the lowest leakage inductance. For the windings, a copper foil is used and the core is made out of

3C90 ferrite. The primary winding is composed of 2 coils connected in series, each containing 14 turns. The secondary winding is composed of 2 coils connected in parallel, each containing 14 turns [8].

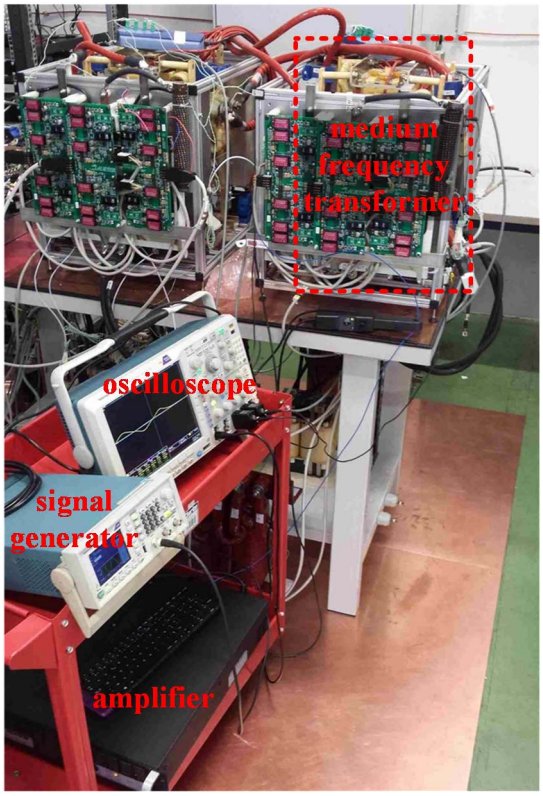

Fig. 3: DC-DC power converter with the medium frequency single-phase transformer as part of experimental setup for measurements of hysteresis loops

The primary winding was supplied with a power amplifier controlled by a signal generator (Table I) under a slow time varying excitation current of 20 A (Θ=560 A). The frequency range between 1 Hz and 100 Hz was considered in order to reduce the dynamic effects in the magnetic material. The hysteresis characteristics $\Phi_c(\Theta)$ was calculated from the set of measured voltages and currents [27], [28]. The flux density was obtained by numerical integration of the voltage induced in the secondary winding. The core was demagnetized before each measurement.

Table I: Equipment used for the measurement of hysteresis loops

Signal generator	Tektronix AFG2021
Amplifier	AE Techron 7224
Current probe	Chauvin Arnoux E3N
Voltage probe	Tektronix TPP0500
Oscilloscope	Tektronix MDO4054B-3

In order to calculate the A_n, $S_{x,n}$, $S_{y,n}$, K_1 and K_3 parameters the Levenberg-Marquardt optimization algorithm [29] was used. In the analysed range of excitation currents it was possible to well approximate the hysteresis nonlinearity by one single term N=1 of the series (3). The values of the hysteresis parameters are presented in Table II.

Table II: Feedback Preisach model parameters

$S_{x,1}$ [A]	$S_{y,1}$ [A]	A_1 [-]	K_1 [-]	K_3 [-]
583,2	10,08	0,00609	2,06e05	-3,97e10

The hysteresis model was applied for the symmetrical major loop as a function of the total ampere-turns Θ. Fig. 4 shows the simulated symmetrical major loop compared with the experimental measurement. The differences between the measured and the simulated hysteresis loops are relatively small.

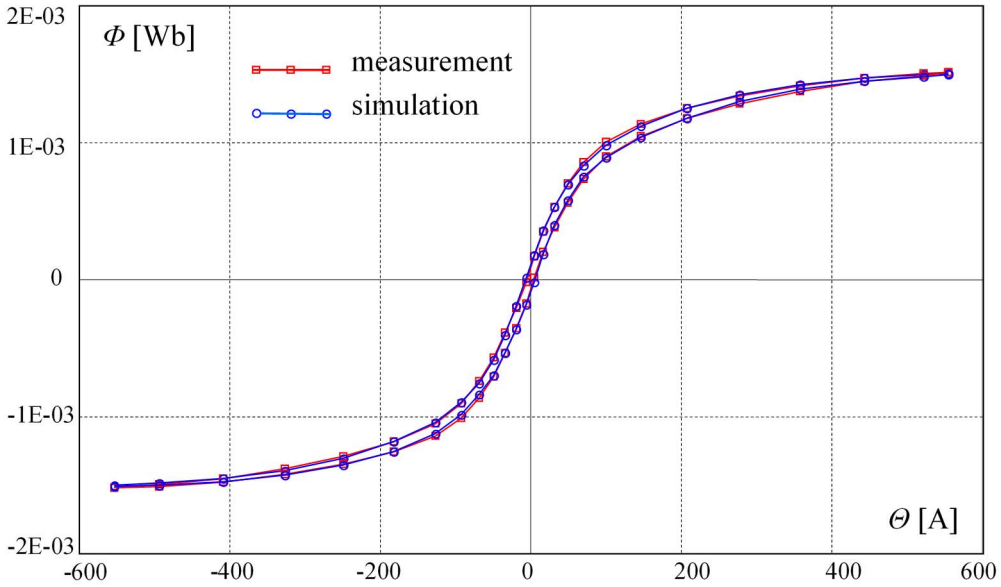

Fig. 4: Simulated and measured trajectories of the symmetrical major hysteresis loops - verification of the hysteresis model

Transformer equivalent circuit

In order to validate the hysteresis model in a circuit simulation, a no load operation of the transformer is considered. The proposed equivalent circuit is presented in Fig. 5. The transformer is supplied from a variable voltage source u_{cc} including a resistance R_0 and an inductance L_0. The resistance of windings R_1 and R_2 is assumed constant in the considered frequency range. The magnetic couplings are modelled with their flux linkages Ψ_1 and Ψ_2. The primary and secondary winding capacitances are modelled with C_1 and C_2 respectively. The primary-secondary capacitance was not included since it is 3 orders of magnitude smaller. The eddy effects and excess losses in the core are modelled with an additional circuit defined by Ψ_3 and R_3 (which may be nonlinear).

The Lagrange energy method is proposed to model the circuit. The generalised coordinates - loop currents are proposed in Fig. 5 and it is assumed that $\dot{q} = \frac{dq}{dt} = i$.

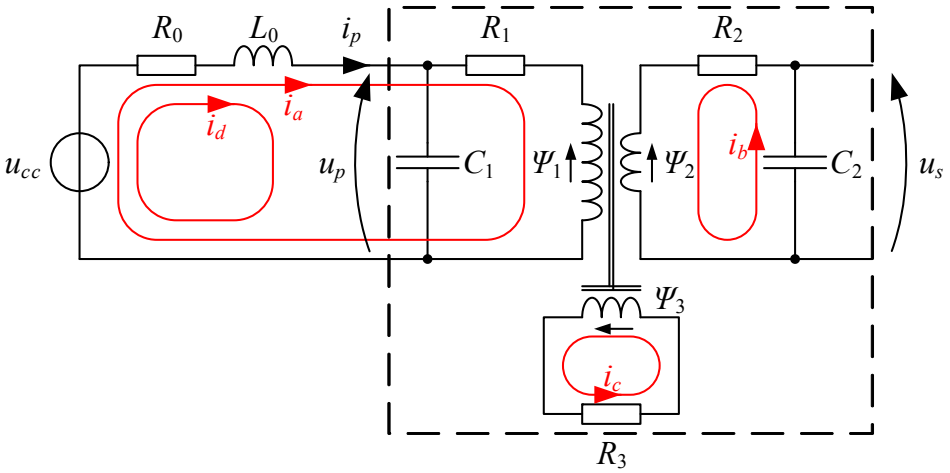

Fig. 5: Transformer equivalent circuit diagram for no load test: u_{cc} - programmable voltage source; R_0, L_0 - resistance and inductance of the voltage source and connections; R_1, C_1, Ψ_1 - primary winding resistance, capacitance and flux linkage; R_2, C_2, Ψ_2 - secondary winding resistance, capacitance and flux linkage; R_3, Ψ_3 - resistance and flux linkage of the equivalent eddy current and excess losses circuit; i_a, i_b, i_c, i_d - loop currents (in red); u_p, u_s, i_p - primary voltage, secondary voltage and primary current

The Lagrange function is defined in the equation (5)

$$\begin{aligned}\mathcal{L}(\dot{q}_a,\dot{q}_b,\dot{q}_c,\dot{q}_d,q_a,q_b,q_c,q_d) &= \left[\frac{1}{2}L_0(\dot{q}_a+\dot{q}_d)^2\right. \\ &+ \left.\int_0^{\dot{q}_a}\Psi_1(\dot{q}_a,\dot{q}_b,\dot{q}_c)\,d\dot{q}_a + \int_0^{\dot{q}_b}\Psi_2(\dot{q}_a,\dot{q}_b,\dot{q}_c)\,d\dot{q}_b + \int_0^{\dot{q}_c}\Psi_3(\dot{q}_a,\dot{q}_b,\dot{q}_c)\,d\dot{q}_c\right] \\ &- \left[\frac{1}{2}\frac{{q_d}^2}{C_1}+\frac{1}{2}\frac{{q_b}^2}{C_2}\right]\end{aligned} \tag{5}$$

and the Rayleigh dissipation function is defined in the equation (6).

$$P_e(\dot{q}_a,\dot{q}_b,\dot{q}_c,\dot{q}_d) = \frac{1}{2}R_0(\dot{q}_a+\dot{q}_d)^2+\frac{1}{2}R_1{\dot{q}_a}^2+\frac{1}{2}R_2{\dot{q}_b}^2+\frac{1}{2}R_3{\dot{q}_c}^2 \tag{6}$$

The Euler-Lagrange equation is defined in (7)

$$\begin{aligned}&\frac{d}{dt}\frac{\partial\mathcal{L}}{\partial\dot{q}_a}-\frac{\partial\mathcal{L}}{\partial q_a}+\frac{\partial P_e}{\partial\dot{q}_a}=u_{cc}(t)\\ &\frac{d}{dt}\frac{\partial\mathcal{L}}{\partial\dot{q}_b}-\frac{\partial\mathcal{L}}{\partial q_b}+\frac{\partial P_e}{\partial\dot{q}_b}=0\\ &\frac{d}{dt}\frac{\partial\mathcal{L}}{\partial\dot{q}_c}-\frac{\partial\mathcal{L}}{\partial q_c}+\frac{\partial P_e}{\partial\dot{q}_c}=0\\ &\frac{d}{dt}\frac{\partial\mathcal{L}}{\partial\dot{q}_d}-\frac{\partial\mathcal{L}}{\partial q_d}+\frac{\partial P_e}{\partial\dot{q}_d}=u_{cc}(t)\end{aligned} \tag{7}$$

which after some simplifications can be transformed to the equation (8).

$$\begin{aligned}&\begin{bmatrix} L_0+\frac{\partial\Psi_1}{\partial\dot{q}_a} & \frac{\partial\Psi_1}{\partial\dot{q}_b} & \frac{\partial\Psi_1}{\partial\dot{q}_c} & L_0\\ \frac{\partial\Psi_2}{\partial\dot{q}_a} & \frac{\partial\Psi_2}{\partial\dot{q}_b} & \frac{\partial\Psi_2}{\partial\dot{q}_c} & 0\\ \frac{\partial\Psi_3}{\partial\dot{q}_a} & \frac{\partial\Psi_3}{\partial\dot{q}_b} & \frac{\partial\Psi_3}{\partial\dot{q}_c} & 0\\ L_0 & 0 & 0 & L_0\end{bmatrix}\begin{bmatrix}\ddot{q}_a\\ \ddot{q}_b\\ \ddot{q}_c\\ \ddot{q}_d\end{bmatrix}\\ &= \begin{bmatrix}u_{cc}(t)\\ 0\\ 0\\ u_{cc}(t)\end{bmatrix}-\begin{bmatrix}R_0+R_1 & 0 & 0 & R_0\\ 0 & R_2 & 0 & 0\\ 0 & 0 & R_3 & 0\\ R_0 & 0 & 0 & R_0\end{bmatrix}\begin{bmatrix}\dot{q}_a\\ \dot{q}_b\\ \dot{q}_c\\ \dot{q}_d\end{bmatrix}-\begin{bmatrix}0 & 0 & 0 & 0\\ 0 & \frac{1}{C_2} & 0 & 0\\ 0 & 0 & 0 & 0\\ 0 & 0 & 0 & \frac{1}{C_1}\end{bmatrix}\begin{bmatrix}q_a\\ q_b\\ q_c\\ q_d\end{bmatrix}\end{aligned} \tag{8}$$

It is assumed for this type of magnetic core that there is a flux common to all windings Φ_c. Thus, the left hand side of the equation (8) can be expressed with (9) [23]

$$\begin{bmatrix}L_0+L_{\sigma1} & 0 & 0 & 0\\ 0 & L_{\sigma2} & 0 & 0\\ 0 & 0 & L_{\sigma3} & 0\\ L_0 & 0 & 0 & L_0\end{bmatrix}\begin{bmatrix}\ddot{q}_a\\ \ddot{q}_b\\ \ddot{q}_c\\ \ddot{q}_d\end{bmatrix}+\frac{\partial\Phi_c}{\partial\Theta}\begin{bmatrix}N_1N_1 & N_1N_2 & N_1N_3 & 0\\ N_2N_1 & N_2N_2 & N_2N_3 & 0\\ N_3N_1 & N_3N_2 & N_3N_3 & 0\\ 0 & 0 & 0 & 0\end{bmatrix}\begin{bmatrix}\ddot{q}_a\\ \ddot{q}_b\\ \ddot{q}_c\\ \ddot{q}_d\end{bmatrix} \tag{9}$$

where Θ is the total ampere-turns of all coils defined in the equation (10), N_k is the number of turns of the k-th coil and $L_{\sigma k}$ is the leakage inductance.

$$\Theta(\dot{\boldsymbol{q}}) = N_1\dot{q}_a + N_2\dot{q}_b + N_3\dot{q}_c \tag{10}$$

The relationship $\Phi_c(\Theta)$ involves the feedback Preisach model of hysteresis presented in the previous paragraphs.

Circuit simulations and comparison with a measurement

The transformer circuit model involving the feedback Preisach model of hysteresis can be implemented in any nonlinear differential equation computation software. The voltage supply was modelled with a trapezoidal waveform with a variable slope corresponding to the average inverter dv/dt. The model parameters presented in Table III were measured on the prototype transformer.

Table III: Transformer equivalent circuit parameters

	Primary winding	Secondary winding
Number of turns	$N_1 = 28$	$N_2 = 14$
Resistance	$R_1 = 9{,}5$ mΩ	$R_2 = 1{,}9$ mΩ
Inductance	$L_{\sigma 1} = 1{,}3$ µH	$L_{\sigma 2} = 0{,}8$ µH
Capacitance	$C_1 = 0{,}4$ nF	$C_2 = 4{,}3$ nF

A no load operating point at 800 V 17 kHz is presented in Fig. 6 for the simulation and the measurement. A no load operation with an increased supply voltage is presented in Fig. 7 and the simulated hysteresis loops are presented in Fig. 8.

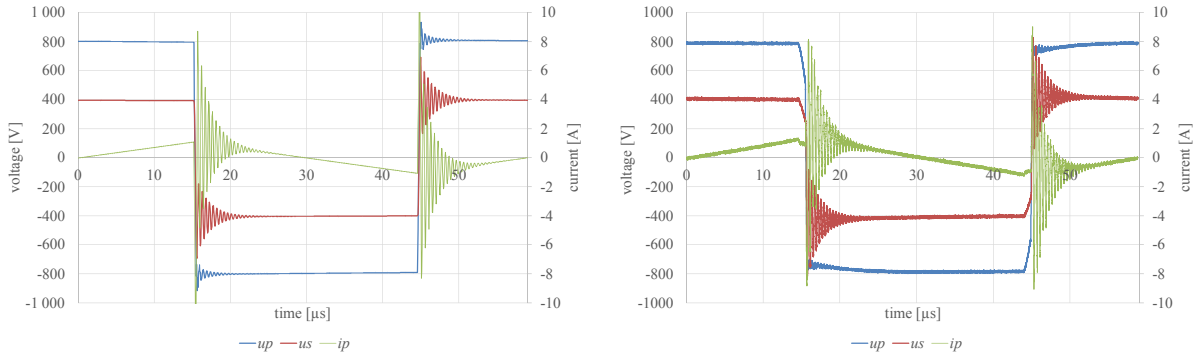

Fig. 6. Simulated (left) and measured (right) waveforms at 800 V 17 kHz no load operation: primary voltage u_p, secondary voltage u_s, primary current i_p

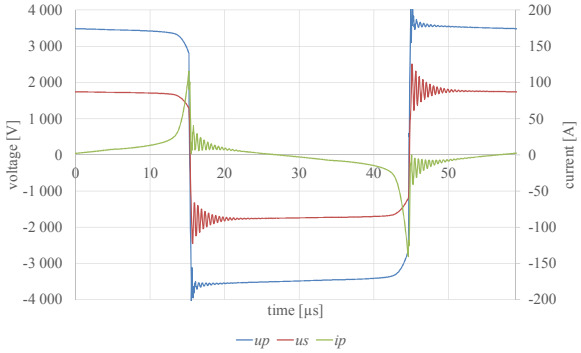

Fig. 7. Simulated waveforms with an increased supply voltage 3500 V 17 kHz no load operation: primary voltage u_p, secondary voltage u_s, primary current i_p

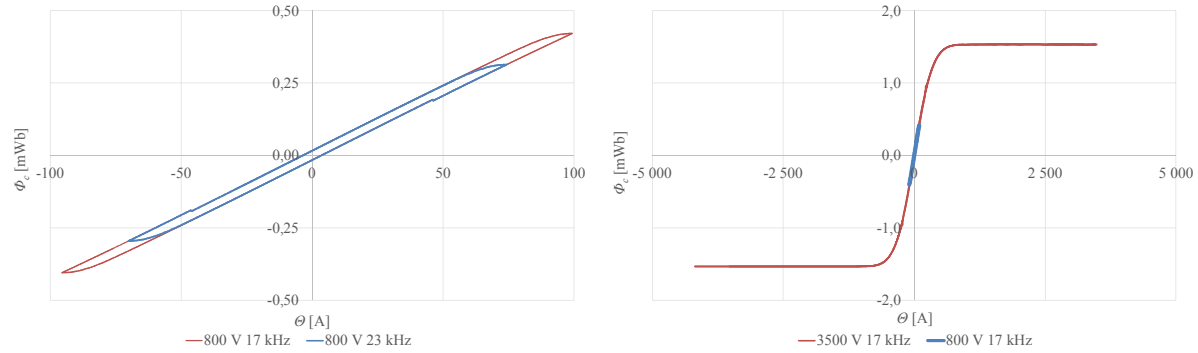

Fig. 8. Simulated hysteresis loops at 800 V 17 kHz and 23 kHz (left) and with an increased supply voltage 3500 V 17 kHz compared with 800 V 17 kHz (right): flux common to all windings Φ_c, total ampere-turns of all coils Θ

It can be observed that the simulation model fits the measurement quite well. The small differences are probably caused by the slightly different supply voltage shape. The transformer circuit model involving

the feedback Preisach model of hysteresis enables a precise analysis in various operating conditions like frequency change or supply voltage shape change. The hysteresis and eddy current losses are directly calculated enabling, for example to evaluate the impact of a power converter design on the transformer performance.

Conclusions

This article presents a precise modelling method of a medium frequency single-phase transformer. The feedback Preisach model of hysteresis is developed and implemented in an equivalent circuit simulation. The circuit model parameters are identified for a high power and high efficiency DC-DC converter prototype. The modelled hysteresis loops are compared against a measurement. A no load operation of the transformer is analysed with a voltage source inverter supply. The presented simulation results are compared against a measurement showing a good fit.
The proposed transformer modelling method has been proven in the analysis of a DC-DC converter operation. The method can be used in a design process of power converters and in health monitoring of medium frequency transformers thanks to its accurate losses estimation in various operation conditions. The model can be further developed including a precise model of winding resistance and a more detailed model of winding capacitances.

References

[1] Meah, K., Ula, S., *Comparative Evaluation of HVDC and HVAC Transmission Systems*, IEEE Power Engineering Society General Meeting, 2007

[2] Millan, J., Godignon, P., Perpina, X., Perez-Tomas, A., Rebollo, J., *A Survey of Wide Bandgap Power Semiconductor Devices*, IEEE Transactions on Power Electronics, Vol. 29, No. 5, May 2014

[3] Walker, G. R., Sernia, P. C., *Cascaded DC-DC converter connection of photovoltaic modules*, IEEE Transactions on Power Electronics, 2004

[4] Du, Y., Lukic, S., Jacobson, B., Huang, A., *Review of high power isolated bi-directional DC-DC converters for PHEV/EV DC charging infrastructure*, IEEE Energy Conversion Congress and Exposition, Phoenix AZ, USA, 2011

[5] De Prada Gil, M., Dominguez-Garcia, J.L., Diaz-Gonzalez, F., Aragues-Penalba, M., Gomis-Bellmunt, O., *Feasibility analysis of offshore wind power plants with DC collection grid*, Renewable Energy, vol. 78, pp. 467–477, 2015

[6] Farnesi, S., Marchesoni, M., Vaccaro, L., *Advances in Locomotive Power Electronic Systems Directly Fed Through AC Lines*, International Symposium on Power Electronics, Electrical Drives, Automation and Motion, Anacapri, Italy, 2016

[7] DeDoncker, R. W., Kheraluwala, M. H., Divan, D. M., *Power conversion apparatus for DC/DC conversion using dual active bridges*, US patent US5027264A, 1991

[8] Pereira, A., Lefebvre, B., Sixdenier, F., Raulet, M. A., Burais, N., *Comparison Between Numerical and Analytical Methods of AC Resistance Evaluation for Medium Frequency Transformers: Validation on a Prototype*, IEEE Electrical Power and Energy Conference, London ON, Canada, 2015

[9] Wilk, A., *Representation of magnetic hysteresis in a circuit model of a single-phase transformer*, The International Journal for Computation and Mathematics in Electrical and Electronic Engineering, Vol. 34 Iss 3 pp. 778 - 791, 2015

[10] Liorzu, F., Phelps, B., Atherton, D.L., *Macroscopic models of magnetization*, IEEE Transactions On Magnetics, Vol. 36, No. 2, pp. 418-428, 2000

[11] Preisach, F., *Über die magnetische Nachwirkung*, Zeitschrift für Physik, Bd.94, 1935, pp. 274-302, 1935

[12] Jiles, D.C. and Atherton, D.L., *Ferromagnetic hysteresis*, IEEE Transactions on Magnetics, Vol. 19 No. 5, pp. 2183-2185, 1983

[13] Łyskawiński, W., Sujka, P., Szeląg, W., and Barański, M., *Numerical analysis of hysteresis loss in pulse transformer*, Archives of Electrical Engineering, Vol. 60(2), pp. 187-195, 2011

[14] Jędryczka, C., Sujka, P., and Szeląg, W., *The influence of magnetic hysteresis on magnetorheological fluid clutch operation*, COMPEL: The International Journal for Computation and Mathematics in Electrical and Electronic Engineering, Vol. 26 No. 2, pp. 711-721, 2009

[15] Gyselinck, J., Dular, P., Sadowski, N., Leite, J. and Bastos, J., *Incorporation of a Jiles-Atherton vector hysteresis model in 2D FE magnetic field computations*, COMPEL: The International Journal for Computation and Mathematics in Electrical and Electronic Engineering, Vol. 23 No. 3, pp. 685-93, 2004

[16] Knypiński, Ł., Nowak L., Sujka, P. and Radziuk K, *Application of a PSO algorithm for identification of the parameters of Jiles-Atherton hysteresis model*, Archives of Electrical Engineering, Vol. 61(2), pp. 139-148, 2012

[17] Krasnosel'skii, M.A., and Pokrovskii, A.V, *Sistemy s gisterezisom (Systems with Hysteresis)*, Nauka, Moskow, 1983

[18] Mayergoyz, I.D, *Mathematical models of hysteresis*, IEEE Transactions on Magnetics, Vol. MAG-22, No. 5, pp. 603-608, 1986

[19] Iványi, A., Füzi, J., and Szabó, Z, *Preisach models of ferromagnetic hysteresis*, Electrical Review (Poland), R. LXXIX 3/2003, pp. 145-150, 2003

[20] Brokate, M., and Della Tore E., *The wiping-out property of the moving model*, IEEE Transactions on Magnetics, Vol. 27 No. 5, pp. 3811-3814, 1991

[21] Kadar, G., and Della Torre E., *Hysteresis modeling I: Noncongruency*, IEEE Transactions on Magnetics, Vol. 23, No. 5, pp. 2820-2822, 1987

[22] Wilk, A., *Internal winding fault detection in a traction transformer using a real-time reference model*, Electromotion, Vol. 17, No. 1, pp. 37-46, 2010

[23] Wilk, A., Nieznanski, J., Moson, I., *Nonlinear model of a wound iron core traction transformer with the account of magnetic hysteresis*, XIX International Conference on Electrical Machines (ICEM-2010), Rome, Italy, 7 pp, 2010

[24] Mayergoyz, I.D., and Adly, A.A., *Numerical Implementation of the feedback Preisach model*, IEEE Transactions on Magnetics, Vol. 28, No. 5, pp. 2605-2607, 1992

[25] Della Torre, E., and Vajda, F., *Parameter identification of the complete-moving-hysteresis model using major loop data*, IEEE Transactions on Magnetics, Vol. 30 No. 6, pp. 3811-3814, 1994

[26] Ragusa, C., *An analytical method for the identification of the Preisach distribution function*, Journal of Magnetism and Magnetic Materials, 254-255, pp. 259–261, 2003

[27] Dolinar, M., Dolinar, D., Štumberger, G., Polajžer, B., and Ritonja, J., *A three-phase core-type transformer iron core model with included magnetic cross saturation*, IEEE Transactions on Magnetics, Vol. 42, No. 10, pp. 2849-2851, 2006

[28] Fuchs, E.F., and You,Y., *Measurement of λ-i characteristics of asymmetric three-phase transformers and their applications*, Proc. Ninth International conference on Harmonics and Quality of Power, Orlando, Florida, USA, pp. 91-96, 2000

[29] More, J.J., *The Levenberg-Marquardt algorithm: Implementation and theory*, Lecture Notes in Mathematics, Numerical Analysis, 630, pp. 105-116, 1978